Identification of high-K rotation in ^{130}Ba: Testing the consistency of electromagnetic observables

Y. H. Qiang,[1,2,3] C. M. Petrache,[4,*] S. Guo,[1,*] P. M. Walker,[5] D. Mengoni,[6] Q. B. Chen,[7] B. F. Lv,[4] A. Astier,[4] E. Dupont,[4] M. L. Liu,[1] X. H. Zhou,[1] J. G. Wang,[1] D. Bazzacco,[6] A. Boso,[6] A. Goasduff,[6] F. Recchia,[6] D. Testov,[6] F. Galtarossa,[8] G. Jaworski,[8] D. R. Napoli,[8] S. Riccetto,[8] M. Siciliano,[8] J. J. Valiente-Dobon,[8] C. Andreoiu,[9] F. H. Garcia,[9] K. Ortner,[9] K. Whitmore,[9] B. Cederwall,[10] E. A. Lawrie,[11] I. Kuti,[12] D. Sohler,[12] T. Marchlewski,[13] J. Srebrny,[13] A. Tucholski,[13] A. C. Dai,[14] and F. R. Xu[14]

[1]*Institute of Modern Physics, Chinese Academy of Sciences, Lanzhou 730000, China*
[2]*School of Nuclear Science and Technology, Lanzhou University, Lanzhou 730000, China*
[3]*Graduate University of Chinese Academy of Sciences, Beijing 000049, China*
[4]*Centre de Sciences Nucléaires et Sciences de la Matière, CNRS/IN2P3, Université Paris-Saclay, Bât. 104-108, 91405 Orsay, France*
[5]*Department of Physics, University of Surrey, Guildford GU2 7XH, United Kingdom*
[6]*Dipartimento di Fisica e Astronomia dell'Universit, and INFN, Sezione di Padova, 35131 Padova, Italy*
[7]*Physik-Department, Technische Universität München, D-85747 Garching, Germany*
[8]*INFN Laboratori Nazionali di Legnaro, 35020 Legnaro (Pd), Italy*
[9]*Department of Chemistry, Simon Fraser University, Burnaby, BC V5A 1S6, Canada*
[10]*KTH Department of Physics, S-10691 Stockholm, Sweden*
[11]*iThemba LABS, National Research Foundation, PO Box 722, 7131 Somerset West, South Africa*
[12]*Institute for Nuclear Research, Hungarian Academy of Sciences, H-4026 Debrecen, Hungary*
[13]*Heavy Ion Laboratory, University of Warsaw, 02-093 Warsaw, Poland*
[14]*Department of Technical Physics, Peking University, Beijing 100871, People's Republic of China*

(Received 24 September 2018; published 8 January 2019)

The band built on the $K^\pi = 8^-$, $T_{1/2} = 9.4$ ms isomer of ^{130}Ba has been identified, filling the gap in the systematics of the dipole bands built on the 8^- isomers in the $N = 74$ isotones from ^{128}Xe to ^{138}Gd. The use of the GALILEO array in conjunction with its ancillaries EUCLIDES and Neutron Wall, helped to firmly place the newly identified transitions on top of the long-lived isomer. The extracted g_K and g_R gyromagnetic factors are in agreement with the $7/2^+[404] \otimes 9/2^-[514]$ two-neutron Nilsson configuration. Particle-rotor model calculations give an understanding of the limited degree of K mixing. The experimental information on the $K^\pi = 8^-$ isomer of ^{130}Ba is now the most complete among the K isomers of the $N = 74$ isotones.

DOI: 10.1103/PhysRevC.99.014307

I. INTRODUCTION

Isomers provide detailed probes of nuclear structure [1]. For example, on account of their extended half-lives, there are possibilities to measure accurately their electromagnetic moments [2]. For K isomers in deformed nuclei, there is the added feature that their associated rotational bands have moments of inertia and γ-ray branching ratios that further constrain the interpretation of the gyromagnetic ratios and quasiparticle configurations involved.

In the study of K isomers, the sequence of $N = 74$ isotones is remarkable in that all the even-even nuclides from ^{128}Xe to ^{140}Dy have $K^\pi = 8^-$ isomers, with excitation energies ranging from 2.2–2.8 MeV, and with half-lives from 73 ns to 9.4 ms [3]. Of these, only the ^{130}Ba isomer has a measured electric quadrupole moment [4], and only the ^{128}Xe and ^{130}Ba isomers have measured magnetic dipole moments [5]. Furthermore, among the $N = 74$, $K^\pi = 8^-$ isomers, only ^{130}Ba and ^{140}Dy have no identified rotational-band structure, with ^{140}Dy being at the limit of experimental accessibility. There is therefore a special imperative to measure the rotational-band structure associated with the $K^\pi = 8^-$ isomer of ^{130}Ba, and in such a way uniquely to open up the comparison of the full set of observables. In particular, from the measured angular correlations we can extract the mixing ratios, δ, for the transitions, and hence deduce the $B(E2; \Delta I = 1)/B(E2; \Delta I = 2)$ ratios and compare them with the calculated values. We can obtain precise values for the g_K and g_R factors, and test for K mixing in the band built on the isomer. In addition, the g_K value probes the quasiparticle configuration of the isomer. This is what we report in the present work.

The $K^\pi = 8^-$ isomer of ^{130}Ba was first reported in 1966 by Brinckmann *et al.* [6] using the ^{122}Sn(^{12}C, 4n) reaction. The decay of the isomer has been studied using conversion electron and γ spectroscopy most recently by Perkowski *et al.* [7], while the magnetic dipole and static electric quadrupole moments have been measured by Moore *et al.* using collinear laser spectroscopy [8]. The most recent study of the high-spin states of ^{130}Ba has been reported by Kaur *et al.* [9]. However, there have been no previous reports of the rotational structure based on the 8^- isomer.

*Corresponding authors: petrache@csnsm.in2p3.fr; gs@impcas.ac.cn

The $K^{\pi} = 8^-$ isomers of the other $N = 74$ nuclei have been studied by Orce *et al.* [10] for ^{128}Xe, Paul *et al.* [11] and Perkovski *et al.* [12] for ^{132}Ce, Petrache *et al.* [13] and Perkovski *et al.* [14] for ^{134}Nd, Regan *et al.* [15] for ^{136}Sm, Bruce *et al.* [16] and Cullen *et al.* [17] for ^{138}Gd, and Królas *et al.* [18] and Cullen *et al.* [19] for ^{140}Dy. The systematics and theoretical interpretation of the 8^- isomers in the $N = 74$ isotones was recently presented in Refs. [16,20,21].

II. EXPERIMENTAL DETAILS AND RESULTS

The ^{130}Ba nucleus was populated via the ^{122}Sn(^{13}C, $5n$) reaction at a beam energy of 65 MeV. The ^{13}C beam of 5 pnA was provided by the XTU Tandem accelerator of the Laboratori Nazionali di Legnaro. The target consisted of a stack of two self-supporting ^{122}Sn foils with a thickness of 0.5 mg/cm^2 each. The γ rays were detected by the GALILEO spectrometer, which consisted of 25 Compton-suppressed Ge detectors placed on four rings at 90° (ten detectors), 119° (five detectors), 129° (five detectors), and 152° (five detectors). To distinguish different reaction channels, charged particles and neutrons were detected by the EUCLIDES silicon apparatus [22] and the Neutron Wall array [23,24], respectively.

Data were recorded by the GALILEO data acquisition system, which was designed for the GALILEO-EUCLIDES-Neutron Wall Experiment [25]. The accumulated data were unfolded and sorted into files in ROOT format, while Doppler shifts were corrected using a recoil velocity $\beta = v/c = 0.0095$ determined from the present experiment. A total of 1.2×10^9 triple- or higher-fold events have been collected. The coincidence events were sorted into a three-dimensional histogram (cube) and the analysis was carried out with the RADWARE software package [26,27]. A series of two-dimensional histograms (matrices) were also built in coincidence with different sets of detected particles (e.g., $p, \alpha, n, 2n, pn, \alpha n$, etc.), which helped to assign new transitions to different reaction channels or long-lived isomers, and to eliminate and identify contaminants. The ^{130}Ba nucleus was one of the most intensely populated via the $5n$ reaction channel, with about 40% of the fusion-evaporation cross section calculated with the PACE4 code [28].

A two-point angular-correlation ratio, $R_{\rm ac}$ [29], using the detectors placed at 90° and 152°, was employed to deduce the transition multipolarities. The mixing ratios (δ) of the $M1/E2$ transitions were deduced from the transition intensities measured at the four angles available in the GALILEO array (see above), and employing a method developed by Matta [30,31] for the analysis of angular-distribution measurements. For many transitions there are two solutions for δ in the χ^2 plot, with the absolute values larger than 1, and smaller than 1. For all transitions analyzed in the present work, the δ values smaller than 1 have been adopted since they have smaller χ^2 values. Still, we cannot completely exclude the larger values only by angular correlation or distribution measurements. However, it is unlikely for there to be predominantly $E2$ ($\Delta I = 1$) transitions in dipole bands, which normally have predominantly $M1$ transitions.

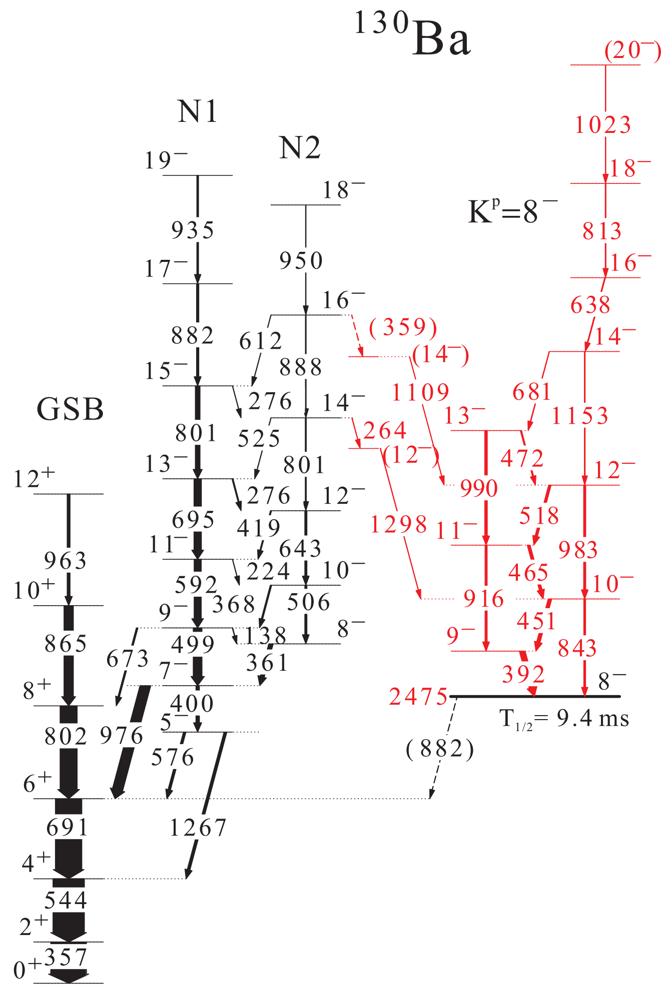

FIG. 1. Partial level scheme of ^{130}Ba. Newly observed structures are marked in red. The energies of the transitions are given in keV, and the widths of the arrows are relative intensities.

A partial level scheme derived from this work is shown in Fig. 1. The details of the newly observed transitions are presented in Table I.

A new structure was established and assigned to populate the previously known 8^- K isomer ($T_{1/2} = 9.4$ ms) [6]. A typical double-gated spectrum for the new structure is shown in Fig. 2(a). The transitions depopulating the isomer were not observed in our measurement since most of the residues in the isomeric state with such a long lifetime were out of the focus of the GALILEO array when they were emitted. A few weak transitions were found, linking the new structure and the previously known band $N2$ [see Fig. 2(b)]. However, the statistics are not enough to safely exclude other possible placements of these weak transitions.

To verify the assignment of the new structure, the coincidences between the γ rays and charged particles and neutrons were examined. Three matrices were built, in which the γ rays are in coincidence with 1α, with one proton, and without detected charged particles, respectively. The γ rays belonging to the new structure are not present in the matrix in coincidence with charged particles (see Fig. 3), indicating that the

TABLE I. Energies, spin and parity assignments, intensities (T_γ), R_{ac} ratios, and mixing ratios (δ) of the transitions in the structure above $K^\pi = 8^-$ isomer in ^{130}Ba.

E_γ (keV)	$I_i^\pi \to I_f^\pi$	T_γ	R_{ac} ratio	δ
$K^\pi = 8^-$				
391.8	$9^- \to 8^-$	$\geqslant$159	0.27(3)	−0.81(48)
450.5	$10^- \to 9^-$	100(6)	0.31(3)	−0.60(15)
842.6	$10^- \to 8^-$	38(10)	1.16(16)	
464.5	$11^- \to 10^-$	83(5)	0.41(2)	−0.37(6)
915.5	$11^- \to 9^-$	60(3)	1.54(17)	
517.7	$12^- \to 11^-$	69(9)	0.42(3)	−0.39(7)
982.5	$12^- \to 10^-$	59(5)	1.53(10)	
471.7	$13^- \to 12^-$	36(10)	0.41(5)	−0.37(13)
989.8	$13^- \to 11^-$	71(5)	1.48(8)	
681.1	$14^- \to 13^-$	15(2)	0.86(21)	
1153.2	$14^- \to 12^-$	20(4)	1.19(18)	
637.6	$16^- \to 14^-$	25(4)	1.55(22)	
812.9	$18^- \to 16^-$	20(4)	1.93(29)	
1023.1	$(20^-) \to 18^-$	15(2)		
Linking transitions				
1298.0	$(12^-) \to 10^-$	7(2)		
264	$14^- \to (12^-)$			
1109.2	$(14^-) \to 12^-$	24(4)	1.52(27)	
(359)	$16^- \to (14^-)$			

new structure belongs to Ba nuclei produced by evaporation of only neutrons.

To further check the assignment of the observed structure to the 8^- isomer of ^{130}Ba, we extracted the intensities of all $^{118-133}$Ba isotopes populated via xn reaction channels on the enriched (∼98%) ^{122}Sn target and the other Sn contaminants (mainly ^{118}Sn and ^{120}Sn, which have natural abundances

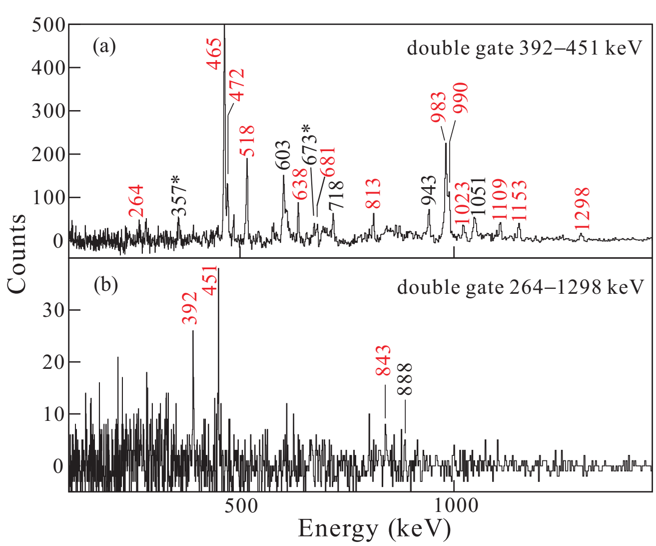

FIG. 2. Double-gated spectra for the new structure built on the 8^- isomer. The γ rays belonging to the new structure are marked in red, while other transitions populating the new structure, not discussed in the present work, are marked in black. The transitions marked with an asterisk are contaminants.

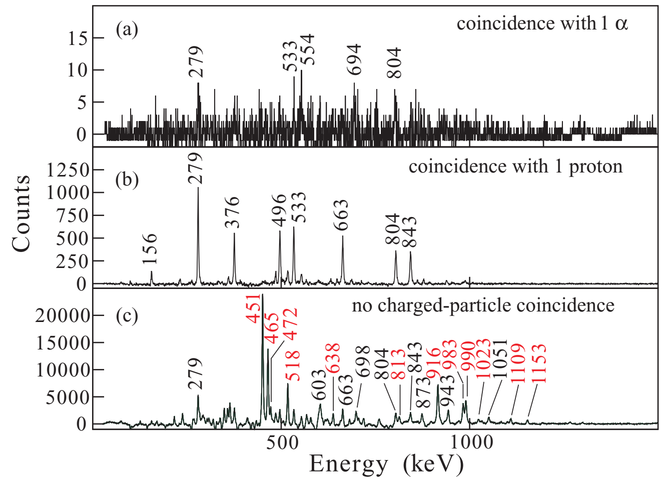

FIG. 3. Spectra gated by the 392-keV γ ray obtained from matrices constructed with different coincidence conditions for the detected charged particles (a): 1α, (b): one proton, (c): no charged particles. The γ rays belonging to the new structure are marked in red.

of 24% and 32%, respectively). Since most transitions of the isotopes other than ^{130,131}Ba are too weak in the total projection spectra, the single-gated spectra were used instead. Spectra obtained by gating on the strongest transition in the isotopes ($2^+ \to 0^+$ for even-even nuclei) were used, and the areas of the strongest peaks in the spectra were extracted ($4^+ \to 2^+$ for even-even nuclei). We obtained the following relative intensities: 100(5) for ^{130}Ba, 74(2) for ^{131}Ba, 3.9(1) for the 8^- isomer of ^{130}Ba, 3.1(1) for ^{132}Ba, 2.0(1) for ^{128}Ba, 1.13(3) for ^{129}Ba, 0.42(1) for ^{126}Ba, and 0.29(2) for ^{127}Ba. The ^{132}Ba and ^{129}Ba were populated via the $3n$ and $6n$ channels in the reaction on ^{122}Sn with 2% and 0.2% relative cross sections (calculated with PACE4), respectively, while the lighter isotopes were produced in the reactions on the ^{118,120}Sn contaminants.

To establish the Ba isotope to which the newly observed structure should be assigned, we built two matrices, one with and one without coincidence with neutrons. The reaction channels associated with the evaporation of a larger number of neutrons are expected to be enhanced in the matrix in coincidence with neutrons. Indeed, as one can see in Fig. 4, the ratios of the peak areas in spectra without and with coincidence with neutrons, are clearly larger for the ^{131}Ba transitions than for the known and new transitions of ^{130}Ba, in agreement with the smaller number of neutrons evaporated in the production of ^{131}Ba ($4n$) than in the production of ^{130}Ba ($5n$). For the transitions belonging to the new structure, the ratios are in the same range of those corresponding to the known transitions of ^{130}Ba. Considering that no coincidences were found between this structure and the ground-state band of ^{130}Ba, the placement of the new structure above the 8^- isomer of ^{130}Ba is the only reasonable explanation.

Apart from ^{130,131}Ba, the new structure is too strongly populated to be associated with any other barium isotope, and it can be safely assigned to ^{130}Ba, rather than ^{131}Ba, based on the coincidence intensities with charged particles and neutrons (Fig. 4) as already discussed.

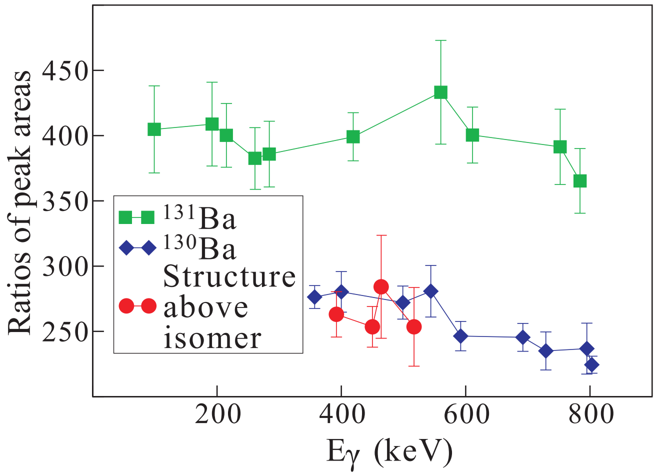

FIG. 4. Ratios of peak areas of selected transitions of ^{131}Ba, ^{130}Ba and of the new structure built on the 8^- isomer, obtained from single-gated spectra on the same γ rays in the matrices without and with coincidence with neutrons. The points correspond to transitions with different energies in the two nuclei.

The energies, initial and final spins and parities, the $E2/M1$ mixing ratios (δ), the $\frac{(g_K-g_R)}{Q_0}$ values, and the $B(E2;\Delta I=1)/B(E2;\Delta I=2)$ branching ratios for the newly observed transitions are presented in Table II. The mixing ratios δ included in the table are obtained from the branching ratios which usually have smaller error bars than those obtained from the angular distributions and correlations, which are needed to get the sign of the mixing ratio. However, the δ values obtained from the two methods agree rather well.

III. DISCUSSION

In the present work the focus is on the high-K part of the level scheme, or, more specifically, the states that decay through the 9.4 ms isomer. First, the K value of the isomer is considered. The usual assumption is that the K value is equal to the spin of the band head, here $K=8$, but this can be tested using the $E2$ components of the $\Delta I=1$ in-band transitions, themselves obtained from the angular-correlation analysis. In Fig. 5 the experimental $B(E2;\Delta I=1)/B(E2;\Delta I=2)$ values are compared to the calculated ones, which, in the

TABLE II. Spin and parity I^π, energies of transitions E_γ(I → I-1), mixing ratios δ_γ(I → I-1), $\frac{(g_K-g_R)}{Q_0}$ values, and $B(E2;\Delta I=1)/B(E2;\Delta I=2)$ ratios of the structure above the $K^\pi=8^-$ isomer in ^{130}Ba.

I^π	E_γ(I → I-1) (keV)	δ_γ(I → I-1)	$\frac{(g_K-g_R)}{Q_0}$ $[(eb)^{-1}]$	$\frac{B(E2;\Delta I=1)}{B(E2;\Delta I=2)}$
9^-	391.8	−0.81(48)		
10^-	450.5	−0.60(15)	-0.080^{+17}_{-11}	16.1(85)
11^-	464.5	−0.37(6)	−0.093(4)	5.2(19)
12^-	517.7	−0.39(7)	−0.101(9)	3.7(21)
13^-	471.7	−0.37(13)	−0.084(14)	2.4(17)

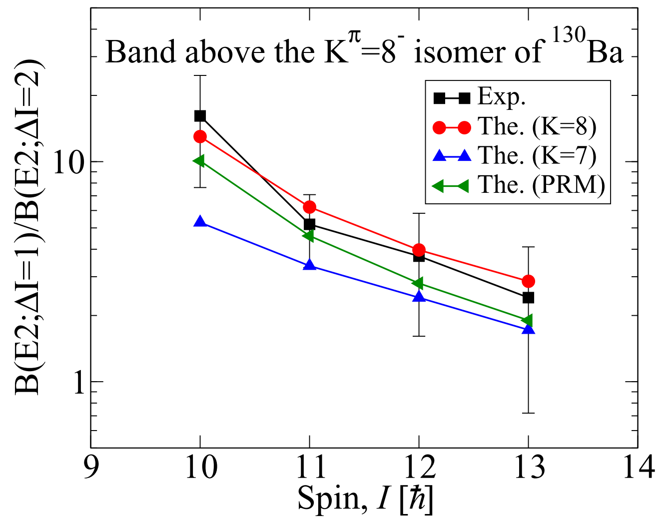

FIG. 5. Comparison of experimental and theoretical $B(E2;\Delta I=1)/B(E2;\Delta I=2)$ ratios of reduced transition probabilities for the band built on the $K^\pi=8^-$ isomer of ^{130}Ba extracted in the present work. The values in red and blue are the theoretical values for $K=8$ ad $K=7$, respectively. One can see the good agreement of the experimental values with the theoretical calculations for $K=8$.

rotational model, are equal to the ratios of the squares of the Clebsch-Gordan coefficients, based on the expression [32]:

$$B(E2, I \to I') = \frac{5}{16\pi} e^2 Q_0^2 \langle I K 20 | I' K \rangle^2, \quad (1)$$

where e is the electronic charge, and Q_0 is the intrinsic quadrupole moment. With $K=8$, very good agreement is obtained, which is a strong argument in favor of a good K value for the isomer. For comparison, the ratios for $K=7$ are seen (Fig. 5) to differ significantly from the experimental data.

Next the g factors are considered. The values of $(g_K - g_R)/Q_0$ for the states above the $K^\pi=8^-$ isomer are obtained from the γ-ray branching ratios and standard formulas [33]:

$$\frac{\delta^2}{1+\delta^2} = \frac{2K^2(2I-1)}{(I+1)(I-1+K)(I-1-K)} \frac{E_1^5}{E_2^5} \frac{T_2}{T_1}, \quad (2)$$

$$\frac{g_K - g_R}{Q_0} = \frac{0.933 E_1}{\delta\sqrt{(I^2-1)}}, \quad (3)$$

where δ is the mixing ratio, E is the transition energy in MeV, T is the γ-ray transition intensity, and Q_0 is in units of eb. The subscripts 1, 2 refer to $\Delta I=1, 2$ transitions, respectively. The sign of δ is obtained from the angular correlations. As it can be seen in Table II, the smallest uncertainty for the values of $(g_K - g_R)/Q_0$ is found for the decay of the $I=11$ band member, and therefore the $(g_K - g_R)/Q_0$ value −0.093(4) for this spin is used in the following. It is consistent with the other values, taking into account their uncertainties. The magnetic dipole moment of $\mu = -0.043(28)\,\mu_N$ and the spectroscopic quadrupole moment of $Q_s = +2.77(30)\,eb$ of the $K^\pi=8^-$ isomer have been measured by Moore et al. [8]. However, Stone [4] renormalized the original quadrupole moment to obtain $Q_s = +2.40(6)\,eb$, which corresponds to an intrinsic quadrupole moment of $Q_0 = +3.42(9)\,eb$, assuming $K = 8$. Adopting this value, and $\mu = -0.043(28)\,\mu_N$, the measured moments enable g_K and g_R to be extracted separately, which is an unusual circumstance, and is unique among the isomers of the $N = 74$ isotones. We obtain $g_K = -0.040(5)$ and $g_R = 0.278(15)$.

Consider first the rotational g factor, $g_R = 0.278(15)$. This is smaller than the simple rotational approximation $g_R = Z/A = 0.43$, while restriction to valence nucleons leads to the same value, $g_R = N_p/(N_p + N_n) = 0.43$ for ^{130}Ba. However, Stone *et al.* [34] have shown that, at least for the $A \approx 180$ region, neutron-dominated multiquasiparticle configurations have smaller g_R values compared to proton-dominated configurations, albeit with considerable uncertainties. Since a two-neutron configuration is expected for the ^{130}Ba isomer (see below), the present g_R value appears to be reasonable. It is notable, however, that the obtained experimental uncertainty is relatively small, and further data of this quality would enable useful testing of model predictions.

Consider next the intrinsic g factor, $g_K = -0.040(5)$. Studies of the other $K^\pi = 8^-$ isomers in the $N = 74$ isotones, from ^{128}Xe to ^{140}Dy, lead consistently to the assignment of the two-neutron, $7/2^+[404] \otimes 9/2^-[514]$ Nilsson configuration. With this configuration, the opposed intrinsic spins of the two neutrons lead to the expectation that $g_K = 0$. However, the $g_K = -0.040(5)$ value for the ^{130}Ba isomer is significantly different from zero. Although the difference is less than typical experimental uncertainties, the small uncertainty in the present case means that the nonzero value requires an explanation. Accordingly, the data are examined for the two component neutrons in the neighboring isotopes.

The nuclide ^{129}Ba has a $7/2^+[404]$ band with known μ and Q_s, and ^{131}Ba has a $9/2^-[514]$ band also with known μ and Q_s [4,5]. There is therefore the same level of completeness for these one-quasiparticle bands as there is for the two-quasiparticle, $K^\pi = 8^-$ band of ^{130}Ba. However, no uncertainties have been reported for the γ-ray branching ratios of the $9/2^-$ band of ^{131}Ba [35]. Therefore, the values have been obtained from the present data set, yielding $g_\Omega = -0.245(8)$ for the $9/2^-[514]$ band of ^{131}Ba.

Byrne *et al.* [36] measured the branching ratios in the $7/2^+[404]$ band of ^{129}Ba. From these and the quadrupole and dipole moments, we obtain $g_\Omega = 0.232(7)$. Then, assuming additivity such that $Kg_K = \Omega_1 g_{\Omega_1} + \Omega_2 g_{\Omega_2}$, the $K^\pi = 8^-$ band would be expected to have $g_K = -0.036(6)$. This is in excellent accord with our value of $g_K = -0.040(5)$ from the ^{130}Ba data. We note that rotation alignment and other possible K-mixing effects in ^{130}Ba are included implicitly by making comparison with the ^{129}Ba and ^{131}Ba experimental values (together with additivity). Nevertheless, the in-band branching ratios show the dominance of $K = 8$, and the semiempirical good-K interpretation is well satisfied.

It is also useful to compare the data with particle-rotor model (PRM) calculations [37,38] and constrained covariant density functional theory [39] to determine the deformation parameters. For the $K^\pi = 8^-$ band head in ^{130}Ba, the deformations obtained are $\beta_2 = 0.23$ and $\gamma = 12^\circ$ using PC-PK1 interaction [40], which compare with $\beta_2 = 0.18$ and $\gamma = 6^\circ$ from earlier total-Routhian-surface calculations [20].

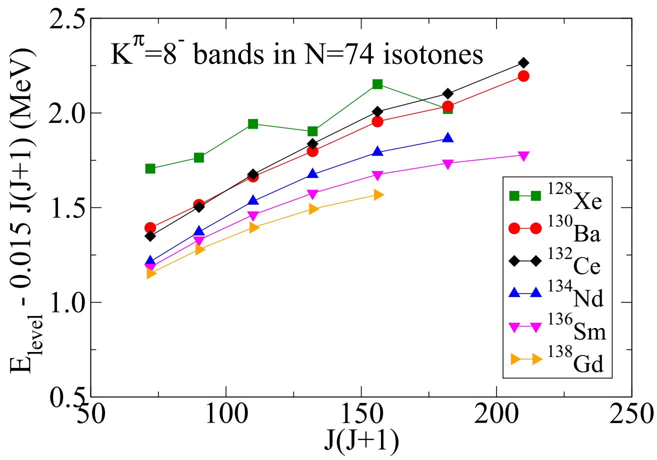

FIG. 6. Energies relative to a rigid rotor for the bands built on the $K^\pi = 8^-$ isomers of the $N = 74$ isotones.

The good angular momentum of the PRM enables a K decomposition, which shows that the band head is 90% $K = 8$, and the model well reproduces the experimental in-band $B(E2)$ ratios, as shown in Fig. 5. In addition, the band-head quadrupole moment is calculated to be $Q_0 = 3.60$ eb, which is close to the experimental value (assuming $K = 8$) of 3.42(9) eb.

The rotational characteristics of the band built on the 8^- isomer have also been investigated. As one can see in Fig. 6, the bands of ^{130}Ba and ^{132}Ce are very similar. The small alignment of $\sim 2\,\hbar$ of the $K^\pi = 8^-$ band of ^{130}Ba (see Fig. 7) is consistent with only a small degree of K mixing. The moment of inertia $J^{(1)}$ is compared to the configuration constrained TRS calculations [41] of the potential energy surface corresponding to the $7/2^+[404] \otimes 9/2^-[514]$ Nilsson configuration in Fig. 8, showing a very good agreement and strongly supporting the assigned configuration.

In summary, we identified the band built on the long-lived $K^\pi = 8^-$ isomer of ^{130}Ba, completing thus the systematics of

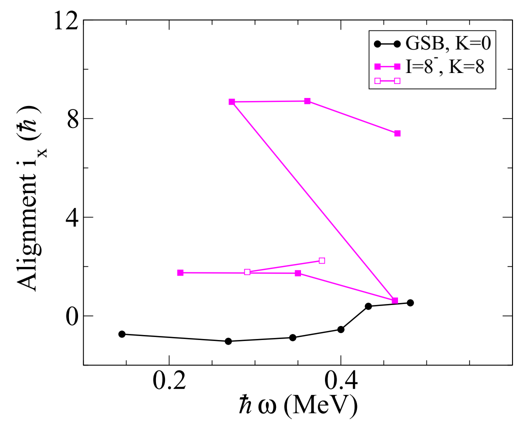

FIG. 7. Experimental quasiparticle alignments for the ground-state band (GSB) and the $K^\pi = 8^-$ band of ^{130}Ba. A reference with $J_0 = 14\,\hbar^2\text{MeV}^{-1}$ and $J_2 = 38\,\hbar^4\text{MeV}^{-3}$ has been subtracted. The adopted K values for the GSB and the $K^\pi = 8^-$ band are 0 and 8, respectively.

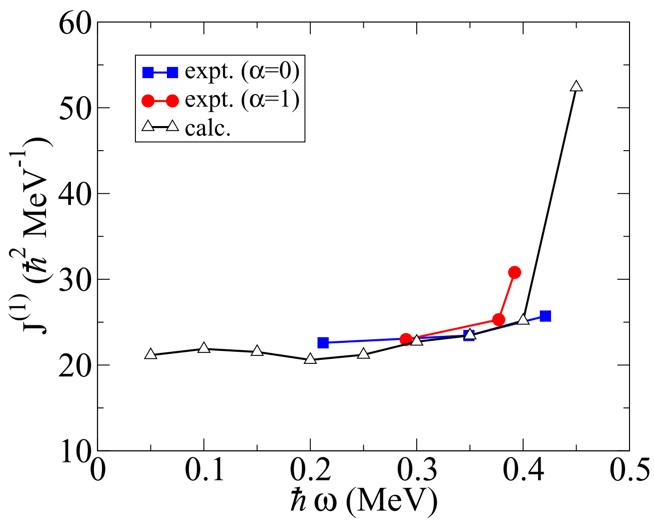

FIG. 8. Moment of inertia $\mathcal{J}^{(1)}$ from TRS calculations for the neutron $g_{7/2}[404]7/2^+ \otimes h_{11/2}[514]9/2^-$ Nilsson configuration in comparison with the experimental $\mathcal{J}^{(1)}$ of the band built on the $K = 8^-$ isomer of ^{130}Ba. The two signature partners with $\alpha = 0, 1$ of the experimental dipole band are drawn with red and black colors. One can see the very good agreement between the experimental and calculated $\mathcal{J}^{(1)}$ values over the entire observed frequency range.

the bands built on the 8^- isomers in the $N = 74$ nuclei from ^{128}Xe to ^{138}Gd. We extracted precise values of the g_K and g_R factors of the assigned $7/2^+[404] \otimes 9/2^-[514]$ Nilsson configuration, and investigated the consistency of the electromagnetic observables of the structure built on the isomer. PRM calculations give useful information about the K purity, consistent with the observed properties. Comparing also with neighboring nuclei, we found a remarkable consistency in the description of the two-neutron configuration assigned to the ^{130}Ba isomer, only possible by using the powerful tools of γ-ray spectroscopy.

ACKNOWLEDGMENTS

This research is supported by the National Natural Science Foundation of China (Grants No. 11505242, No. 11305220, No. U1732139, No. 11775274, and No. 11575255), by the Minister of Europe and Foreign Affairs, Partnership Hubert Curien, project Cai YuanPei 2018, No. 41458XH, by the Natural Sciences and Engineering Research Council of Canada, by the GINOP-2.3.3-15-2016-00034 project in Hungary, by the GINOP-2.3.3-15-2016-00034, National Research, Development and Innovation Office NKFIH, Contract No. PD 124717, by the Polish National Science Centre (NCN) Grant No. 2013/10/M/ST2/00427, and by the National Research Foundation of South Africa, GUN: 93531, 109134. The work of Q.B.C. is supported by Deutsche Forschungsgemeinschaft (DFG) and National Natural Science Foundation of China (NSFC) through funds provided to the Sino-German CRC 110 "Symmetries and the Emergence of Structure in QCD".

[1] G. D. Dracoulis, P. M. Walker, and F. G. Kondev, Rep. Prog. Phys. **79**, 076301 (2016).
[2] G. Neyens, Rep. Prog. Phys. **66**, 633 (2003).
[3] F. G. Kondev, G. D. Dracoulis, and T. Kibédi, At. Data Nucl. Data Tables **103-104**, 50 (2015).
[4] N. J. Stone, At. Data Nucl. Data Tables **111-112**, 1 (2016).
[5] N. J. Stone *et al.*, IAEA Report, INDC(NDS) **0658** (2014).
[6] H. F. Brinkmann, C. Heisera, K. F. Alexander, W. Neubert, and H. Rotter, Nucl. Phys. A **81**, 233 (1966).
[7] J. Perkovski *et al.*, Acta Phys. Pol. B **43**, 273 (2012).
[8] R. Moore *et al.*, Phys. Lett. B **547**, 200 (2002).
[9] N. Kaur *et al.*, Eur. Phys. J. A **50**, 5 (2014).
[10] J. N. Orce, A. M. Bruce, A. Emmanouilidis, A. P. Byrne, G. D. Dracoulis, T. Kibédi, M. Caamaño, H. El-Masri, C. J. Pearson, Zs. Podolyák, P. D. Stevenson, P. M. Walker, F. R. Xu, D. M. Cullen, and C. Wheldon, Phys. Rev. C **74**, 034318 (2006).
[11] E. S. Paul *et al.*, Nucl. Phys. A **619**, 177 (1997).
[12] J. Perkovski *et al.*, Eur. Phys. J. A **42**, 379 (2009).
[13] C. M. Petrache *et al.*, Nucl. Phys. A **617**, 249 (1997).
[14] J. Perkowski, J. Andrzejewski, Ch. Droste, Ł. Janiak, E. Grodner, S. G. Rohoziński, L. Próchniak, J. Srebrny, J. Samorajczyk-Pyśk, T. Abraham, K. Hadyńska-Klęk, M. Kisieliński, M. Komorowska, M. Kowalczyk, J. Kownacki, T. Marchlewski, J. Mierzejewski, P. Napiorkowski, A. Stolarz, A. Korman, and M. Zielińska, Phys. Rev. C **95**, 014305 (2017).
[15] P. H. Regan, G. D. Dracoulis, A. P. Byrne, G. J. Lane, T. Kibédi, P. M. Walker, and A. M. Bruce, Phys. Rev. C **51**, 1745 (1995).
[16] A. M. Bruce, A. P. Byrne, G. D. Dracoulis, W. Gelletly, T. Kibèdi, F. G. Kondev, C. S. Purry, P. H. Regan, C. Thwaites, and P. M. Walker, Phys. Rev. C **55**, 620 (1997).
[17] D. M. Cullen, N. Amzal, A. J. Boston, P. A. Butler, A. Keenan, E. S. Paul, H. C. Scraggs, A. M. Bruce, C. M. Parry, J. F. C. Cocks, K. Helariutta, P. M. Jones, R. Julin, S. Juutinen, H. Kankaanpää, H. Kettunen, P. Kuusiniemi, M. Leino, M. Muikku, and A. Savelius, Phys. Rev. C **58**, 846 (1998).
[18] W. Królas, R. Grzywacz, K. P. Rykaczewski, J. C. Batchelder, C. R. Bingham, C. J. Gross, D. Fong, J. H. Hamilton, D. J. Hartley, J. K. Hwang, Y. Larochelle, T. A. Lewis, K. H. Maier, J. W. McConnell, A. Piechaczek, A. V. Ramayya, K. Rykaczewski, D. Shapira, M. N. Tantawy, J. A. Winger, C.-H. Yu, E. F. Zganjar, A. T. Kruppa, W. Nazarewicz, and T. Vertse, Phys. Rev. C **65**, 031303(R) (2002).
[19] D. M. Cullen *et al.*, Phys. Lett. B **529**, 42 (2002).
[20] F. R. Xu, P. M. Walker, and R. Wyss, Phys. Rev. C **59**, 731 (1999).
[21] Y. Lei, G. J. Fu, and Y. M. Zhao, Phys. Rev. C **87**, 044331 (2013).
[22] D. Testov, Eur. Phys. J. A (to be published).
[23] O. Skeppstedt, H. A. Roth, L. Lindström *et al.*, Nucl. Instrum. Meth. Phys. Res. A **421**, 531 (1999).
[24] J. Ljungvall, M. Palacz, and J. Nyberg, Nucl. Instrum. Meth. Phys. Res. A **528**, 741 (2004).
[25] L. Berti, M. Biasotto, S. Fantinel, A. Gozzelino, M. Gulmini, and N. Toniolo, LNL INFN Annual Report, 93 (2014).
[26] D. Radford, Nucl. Instrum. Meth. Phys. Res. A **361**, 297 (1995).
[27] D. Radford, Nucl. Instrum. Meth. Phys. Res. A **361**, 306 (1995).
[28] A. Gavron, Phys. Rev. C **21**, 230 (1980).

[29] A. Krämer-Flecken, T. Morek, R. M. Lieder, W. Gast, G. Hebbinghaus, H. M. Jäger, and W. Urban, Nucl. Instrum. Meth. Phys. Res. A **275**, 333 (1989).
[30] J. T. Matta *et al.*, Phys. Rev. Lett. **114**, 082501 (2015).
[31] J. T. Matta (private communication).
[32] A. Bohr and B. R. Mottelson, *Nuclear Structure* (World Scientific, Singapore, 1998), Vol. 2.
[33] P. Walker *et al.*, Nucl. Phys. A **568**, 397 (1994).
[34] N. J. Stone, J. R. Stone, P. M. Walker, and C. R. Bingham, Phys. Lett. B **726**, 675 (2013).
[35] R. Ma, Y. Liang, E. S. Paul, N. Xu, D. B. Fossan, L. Hildingsson, and R. A. Wyss, Phys. Rev. C **41**, 717 (1990).
[36] A. P. Byrne *et al.*, Nucl. Phys. A **548**, 131 (1992).
[37] B. Qi, S. Q. Zhang, J. Meng, S. Y. Wang, and S. Frauendorf, Phys. Lett. B **675**, 175 (2009).
[38] Q. B. Chen, B. F. Lv, C. M. Petrache, and J. Meng, Phys. Lett. B **782**, 744 (2018).
[39] J. Meng, *Relativistic Density Functional for Nuclear Structure, International Review of Nuclear Physics* (World Scientific, Singapore, 2016), Vol. 10.
[40] P. W. Zhao, Z. P. Li, J. M. Yao, and J. Meng, Phys. Rev. C **82**, 054319 (2010).
[41] X. M. Fu, F. R. Xu, J. C. Pei, C. F. Jiao, Y. Shi, Z. H. Zhang, and Y. A. Lei, Phys. Rev. C **87**, 044319 (2013).